J. Phycol. **28,** 69–82 (1992)

ULTRASTRUCTURE OF THE FEEDING APPARATUS AND MYONEMAL SYSTEM OF THE HETEROTROPHIC DINOFLAGELLATE *PROTOPERIDINIUM SPINULOSUM*[1]

Dean M. Jacobson[2]

Bigelow Laboratory for Ocean Sciences, West Boothbay Harbor, Maine 04575

and

Donald M. Anderson

Biology Department, Woods Hole Oceanographic Institution, Woods Hole, Massachusetts 02543

ABSTRACT

The feeding veil or pallium of the thecate heterotrophic dinoflagellate Protoperidinium spinulosum *Schiller is a highly vesiculate membranous sac containing several arched, sometimes bifurcated microtubular ribbons. It originates from an internal microtubular basket, passes through a sphincter-like osmiophilic ring located inside the posterior flagellar pore, and emerges from the cell at that pore. The osmiophilic ring is part of an interconnected myonemal system (composed of two striated collars and several striated connectives) that is anchored to the pore plate and to two inward protrusions composed of minute sulcal plates. A related species,* Protoperidinium punctulatum *(Paulsen) Balech, also possesses a microtubular basket/osmiophilic ring complex. Elongate electron-dense bodies within the basket resemble digestive secretory granules found in other protists. Granular, electron-lucent microbodies clustered at the anterior end of the basket may also have a role in prey digestion. Dense membranous whorls observed within a* P. spinulosum *cell preserved as it was preparing to initiate feeding indicate a condensed storage site for pallium membranes. A narrow microtubule-strengthened pseudopodal appendage found in two non-feeding cells constitutes the tow filament that serves as the initial linkage between the dinoflagellate and its food. The structures that constitute the pallium and pallium precursors, described here for the first time, are unlike those of other known protists, although some similarities with the dinoflagellate peduncle are evident. The existence of this unique system of organelles may have important ramifications in the search for evolutionary relationships among protists.*

Key index words: heterotrophic dinoflagellates; microtubules; myonemes; pallium; Protoperidinium punctulatum*;* Protoperidinium spinulosum*; pseudopodia; Pyrrophyta*

Heterotrophic dinoflagellates constitute roughly half of the more than 2000 living dinoflagellate species. These can be divided into two groups: those with naked, soft walls and those that are thecate or armored. The latter group is characterized by the presence of a rigid cellulose wall or theca composed of a series of polygonal plates that are used extensively in dinoflagellate taxonomy. Until recently, the feeding mechanisms of thecate heterotrophic dinoflagellates were unknown. The theca was considered to be a barrier that would restrict the uptake of solid food (Calkins 1901), a notion supported by the lack of visible evidence of food ingestion in cells. Osmotrophy was considered unlikely because the large size of thecate dinoflagellates makes them poor competitors with bacteria for dissolved organic carbon due to surface area:volume considerations (Morey-Gaines and Elbrachter 1987). Recent observations by Gaines and Taylor (1984) and Jacobson and Anderson (1986) have clarified this enigma by demonstrating that thecate heterotrophic dinoflagellates from three genera (*Protoperidinium, Oblea, Zygabikodinium*) feed via a food vacuole external to the theca that takes the form of an enveloping pseudopod (the feeding veil or pallium) that surrounds particulate food (usually colonial diatoms) whose size can far surpass that of the dinoflagellate. During the course of feeding, which typically lasts about 30 min, the prey cytoplasm is liquified within the pallium; consequently, no recognizable food particles are transported within the theca. This behavior was unexpected, because the only extensible feeding structure previously known in dinoflagellates is the peduncle, a slender proboscis-like appendage that pierces prey cells and withdraws intact organelles and cytoplasm into an internal digestive vacuole (e.g. Spero 1982).

Species of *Protoperidinium* have been the subject of ultrastructural investigations in the past (Dodge 1971, Neveux and Soyer 1976), but no internal feeding structures have been identified. To date, the only detailed descriptions of the dinoflagellate pallium have been with light micrographs (Gaines and Taylor 1984, Jacobson and Anderson 1986). The only thecate heterotrophic dinoflagellate species to have a feeding structure revealed, the freshwater dinoflagellate *Peridiniopsis berolinense,* has a peduncle with a complex multi-row microtubular array (Wedemayer and Wilcox 1984). Two other thecate species, the photosynthetic *Ceratium hirundinella* (Dodge and Crawford 1970) and *Prorocentrum micans* (Schnepf and Winter 1990), have a microtubular strand or ribbon, but its involvement in feeding (if

[1] Received 13 June 1991. Accepted 11 October 1991.

[2] Address for reprint requests.

any) has not been determined. Here we document for the first time the unique ultrastructure of the pallium in feeding and non-feeding cells of the thecate heterotrophic dinoflagellate *Protoperidinium spinulosum*. In addition, the feeding apparatus of a non-feeding *Protoperidinium punctulatum* cell is presented for comparison.

MATERIALS AND METHODS

Protoperidinium spinulosum Schiller cells used in this study were selected from laboratory cultures. The dinoflagellate was fed diatoms (including *Leptocylindrus danicus, Eucampia zoodiacus,* and *Chaetoceros* sp.) and cultured in completely full, capped 15-mL polypropylene centrifuge tubes that were slowly rotated end-over-end on a "ferris wheel" apparatus. The dinoflagellate was maintained by diluting aliquots of dinoflagellates and diatoms into fresh f/2 medium (Guillard and Ryther 1962). Additional diatoms were added when cultures became food depleted. All cultures were maintained at 20° C on a 14:10 h LD cycle at approximately 100 $\mu E \cdot m^{-2} \cdot s^{-1}$.

Tube cultures were transferred into Petri dishes in order to locate and isolate feeding and nonfeeding cells with the aid of a dissecting microscope. *Protoperidinium punctulatum* (Paulsen) Balech, which was found in a net tow taken from Vineyard Sound, Massachusetts, was acclimatized by rotating the <80-μm size fraction of the tow plankton in a centrifuge tube filled completely with seawater overnight, allowing immobilized dinoflagellates to resume full motility. Prefeeding cells were obtained by selecting cells performing a characteristic spiralling precapture dance. This distinctive behavior usually persists for a minute or so prior to pseudopod deployment (Jacobson and Anderson 1986).

Two fixation methods were used in transmission electron microscopy (TEM) work. The first technique, used for all but two cells in this study, was employed as a result of the failure of conventional, sequential glutaraldehyde/OsO_4 fixation to preserve the pallium intact. Instead, cells were fixed by introducing them via micropipette to an ice-cold mixture of glutaraldehyde and OsO_4 (2% and 1% final concentrations, respectively) that was buffered with 0.1 M cacodylic acid and osmotically augmented with NaCl (0.43 M final concentration); no calcium was added. This portion of the method was modeled after one developed by R. E. Triemer (pers. commun.) After rinsing in NaCl + buffer, the cells were transferred into drops of liquid 2% agar on glass slides and immersed in cold buffer. After ethanol dehydration, the agar-embedded cells were excised as 1-mm blocks with a sharpened metal spatula while being viewed through a dissecting microscope. These blocks were then placed in centrifuge tubes for Epon/Araldite embedding.

Resin-infiltrated cells were polymerized as flat mounts between slides and cover slips that had been treated with "T-fix" (Sunbeam Appliance Services, Inc.; available through Polysciences, Inc.), which is a Teflon spray (Spector et al. 1981). Cured cells were excised from resin wafers and cemented onto blank resin cylinders for ultramicrotomy with a Sorvall MT-2 ultramicrotome. Formation of ribbons of thin sections, critical for serial section analysis, was facilitated by the application of a thin coat of Tackiwax (Boekel Industries, Inc.) to top and bottom faces of the specimen block (Knobler et al. 1978). Ultrathin sections were collected onto Formvar-coated slot grids. As many as 50 sections could be positioned on two of the four slots on each grid. After post-staining with uranyl acetate and lead citrate, the grids were lightly coated with evaporated carbon. Sections were examined using either a Zeiss 10CA or a Philips 300 transmission electron microscope.

The second fixation protocol was designed to use warm temperatures to stabilize microtubules (with traditional sequential fixation) and tannic acid to enhance membrane contrast (Simionescu and Simionescu 1976). The addition of small amounts of $HgCl_2$ to the initial fixative prevented detachment of the pallium from the feeding cell and was used for feeding and non-feeding cells alike. An initial 30-min fixation in cacodylate-buffered 2% glutaraldehyde/1% tannic acid (Mallinckrodt, Inc.), including 1% saturated aqueous $HgCl_2$ at 20° C, was followed by buffer rinse and a 30-min cacodylate-buffered 1% OsO_4 fixation, also at 20° C. All solutions included NaCl as above. Cells were dehydrated in acetone after agar enrobement and embedded as above in the low-viscosity medium of Spurr (1969). This second protocol was employed for both a feeding and non-feeding cell. Those sections originating from these two cells are labeled in figure legends "+tannin."

Cells of *P. spinulosum* were prepared for scanning electron microscopy by single sequential washes with distilled water and 1% triton X detergent, rinses in distilled water, and fixation in 4% formaldehyde. They were then ethanol dehydrated and CO_2 critical point dried. Cells were imaged with a JEOL U-3 scanning electron microscope. Fluorescence observations were made using a Zeiss inverted microscope with mercury illumination and Zeiss filter set 487706.

RESULTS

All references to lateral polarity assume a dorsal viewpoint. All sections are shown from a ventral, 'frontal' viewpoint so that the cell's left is on the right side of the figure, and vice versa. Because of the complexity of the structures described herein, the reader should refer to the interpretive reconstruction of a feeding cell (Fig. 1) as well as a more detailed reconstruction of the flagellar pore region (Fig. 46).

A variety of organelles are evident in a feeding cell, especially in the peripheral cytoplasm (Fig. 2). Numerous electron-dense laminar structures line the inner surface of the theca. These structures display an alternating thin and wide band pattern with a 10-nm periodicity (Fig. 3). Also situated near the theca are vesicles of varying electron density (Fig. 6) and banded trichocysts (Fig. 4). Two types of storage bodies are evident: electron-dense lipid droplets and the more peripherally located electron-lucent, irregularly shaped bodies. The latter are associated with the laminar structures and are not found posterior of the cingulum. A distinct cluster of microbodylike vesicles is found in the center of the cell (Figs. 2, 5). A single putative autolysosome filled with membrane profiles (Fig. 7) was encountered. Within the large nucleus, one to three nucleoli display a complex internal structure (Fig. 8).

The pallia, or external pseudopodia of five feeding *P. spinulosum* cells, one fixed with tannic acid, all display a similar membranous morphology. This structure is composed of a highly convoluted system of membranous channels and vesicles, the latter either empty or filled with electron-dense material (Fig. 9). Oddly, in some cases the pallium sheet surrounding the prey diatom lacks an inner limiting membrane. In one specimen, an inner membrane is present; note also the degraded condition of the prey cytoplasm (Fig. 12, asterisks). The pallium has spread to a very thin sheath (with a thickness of 150 nm) around a *Chaetoceros* spine (Fig. 10). Thin, 5-nm filaments are found within this sheath. In one cell

the obliquely sectioned stalk region of the pallium is solidly filled with a cytoplasmlike matrix (Fig. 11). The stalk of another pallium is decorated with filaments that are associated with periodic bands (each 30 nm wide) present on the inner surface of the pallium membrane (Fig. 13). These bands are seen also in a glancing longitudinal section (Fig. 14).

In the midst of the membranous reticulum of the pallium, several microtubular ribbons radiate from the origin of the pallium at the flagellar pore (Figs. 9, 12). These ribbons may become bifurcate (Fig. 15) and are associated with microfilaments that seem to bind the individual microtubules together.

Besides the pallium itself, the most conspicuous feature of feeding cells is an oblong cytoplasmic compartment, the microtubular basket (MB), which is continuous with the pallium at the flagellar pore (Figs. 9, 35). The periphery of the MB is complex (Figs. 16–19). In places it is composed of three layers: an inner, parallel array of microtubules (center-to-center distance = 45 nm), an amorphous electron-dense layer closely associated with the MB membrane, and an outer array of membranous invaginations with a 30- to 40-nm diameter and a center-to-center distance of 60–80 nm. The inner and outer arrays are not parallel but are angled approximately 30° from each other, as shown in a tangential section of the compartment's dorsal face (Fig. 22), with the microtubular array oriented parallel to the long axis of the MB. The electron-dense layer occurs adjacent to the microtubular layer, although microtubules often extend beyond the electron-dense layer (Figs. 18, 19). This sheath-like layer is most pronounced at the base of the MB (Fig. 23) and is striated. These striations are most evident at an area of localized thickening of the sheath. The MB in some cells is embedded within the cytoplasm (Figs. 2, 20, 23, 25) but can be surrounded by a vacuole, termed the pallial vacuole (PV) (Figs. 16, 24).

The MB is not a closed cytoplasmic compartment. Rather, it opens at its apex adjacent to the ventral-right quarter of the nucleus. The walls of the MB fold back on themselves, principally on the dorsal side facing the sac pusule (Fig. 20). The microtubular ribbon extends only a short distance along the recurved flap. The flap continues as an indistinct, presumably microfilamentous layer (Fig. 21). Several mitochondria (or quite likely, a single anastomosing mitochondrion) reside in the region directly beneath the apical flap (Figs. 20, 21).

The contents of the MB (which we term the "pallioplasm") vary somewhat in appearance among several comparably fixed cells but always lack such widely distributed organelles as mitochondria and endoplasmic reticulum. In cells that are attached to diatoms whose cytoplasm is in an advanced stage of degradation, the pallioplasm is less dense than that of a cell whose prey cytoplasm was still relatively intact (compare Fig. 19 with Fig. 17). Further, two cells attached to well-digested diatoms have lipid-like electron-dense droplets in the pallium and pallioplasm (Figs. 12, 20, 21, 35). Elongate electron-dense bodies were observed in one nonfeeding cell (Fig. 24) and in *P. punctulatum* (Fig. 23).

In light microscopic auto-fluorescence observations of live *P. spinulosum* cells, the cytoplasm fluoresces a brilliant, uniform green with dark regions corresponding to the sac pusule and nucleus (Jacob-

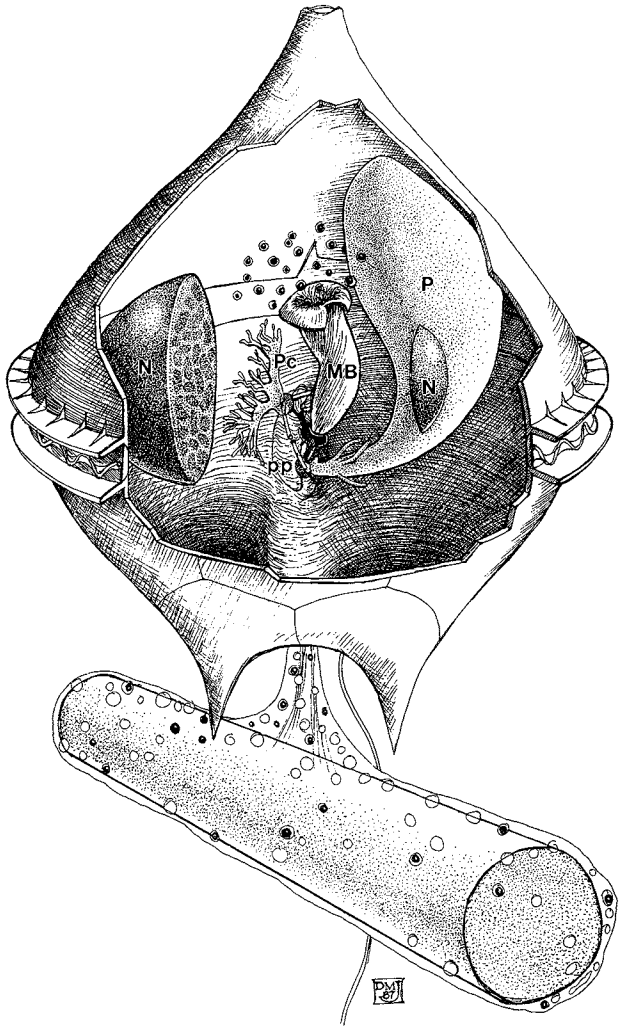

NOTE: Scale bars represent 1.0 μm unless otherwise noted. Abbreviations used: a = anterior sulcal plate; AASP = anterior accessory sulcal plate; bb = basal body; C = corona of MB; fl = fibrillar lamellae; l = left sulcal plate; LF, LB = longitudinal flagellum and basal body; LMR = longitudinal microtubular root; m = mitochondria; MB = microtubular basket; N = nucleus; p = posterior sulcal plate; P = sac pusule; PASP = posterior accessory sulcal plates; Pc = collecting pusule; pp = pore plate; PS = pallial sphincter; r = right sulcal plate; PV = pallial vacuole; R = microtubular ribbon; SC = striated collar (sphincters of pusules); T = thecal plate; TF, TB = transverse flagellum and basal body.

FIG. 1. Diagrammatic reconstruction of *Protoperidinium spinulosum* (three-quarter dorsal view) feeding on a cylindrical diatom showing arrangement of relevant organelles. Nucleus has been mostly cut away to reveal pusules and the microtubular basket.

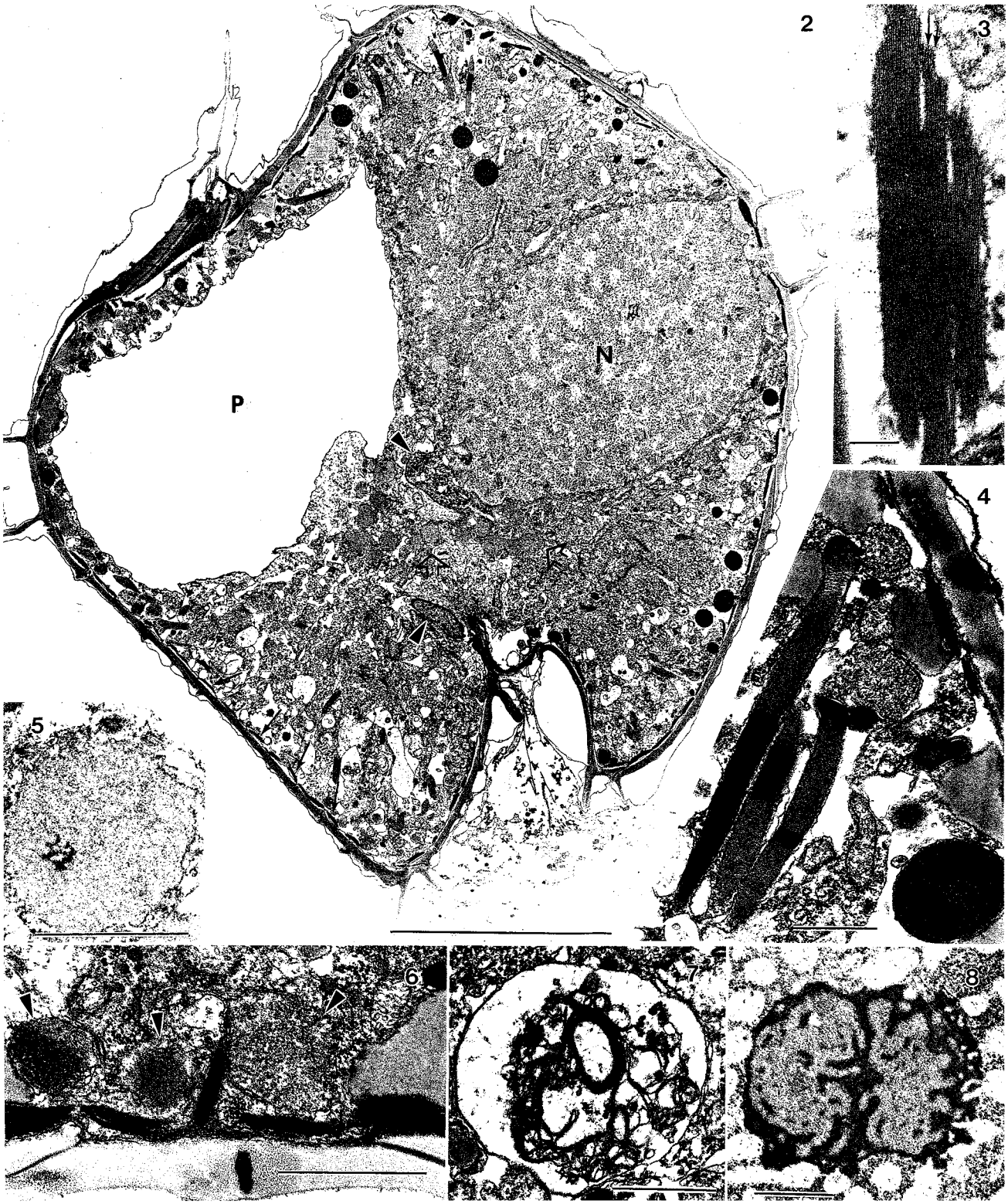

FIGS. 2–8. General cytology of *Protoperidinium spinulosum*. FIG. 2. Longitudinal section of feeding cell. Arrowheads show upper and basal portion of MB. Open arrows indicate microbody cluster. Small arrows (lower left) indicate lamellar bodies. Scale bar = 10 μm. FIG. 3. Lamellar body, with membrane-like lamellae (arrows). Scale bar = 100 nm. FIG. 4. Other peripheral organelles, including trichocysts and storage bodies. FIG. 5. Microbody near MB (see Fig. 2). FIG. 6. Subthecal vesicles (arrowheads). FIG. 7. Putative autolysosome in peripheral cytoplasm. FIG. 8. Nucleolus.

FIGS. 9–15. The pallium of *Protoperidinium spinulosum*. FIG. 9. Longitudinal section with pallium surrounding the diatom *Eucampia zoodiacus* (asterisk). Note ribbon of microtubules, the MB and the pallial sphincter and corona. FIG. 10. Pallium extension surrounding hollow spine of *Chaetoceros* sp. Note microfilaments (arrow). FIG. 11. Oblique section of pallium stalk adjacent to the pallial sphincter (glancing section) and corona. FIG. 12. Transverse section of antapical horns of *P. spinulosum*. An inner membrane (arrows) surrounds *Eucampia zoodiacus* frustules (asterisks). Note electron-dense droplets in pallium, arched microtubular ribbons, and the highly degraded condition of the diatom cytoplasm. FIG. 13. Proximal stalk region of pallium showing periodic densities on inside of membrane (dash marks) and outer fringe of filaments (arrow). FIG. 14. Glancing tangential section of pallium stalk membrane showing regularly spaced transverse bands. FIG. 15. Bifurcated microtubular ribbon in pallium stalk.

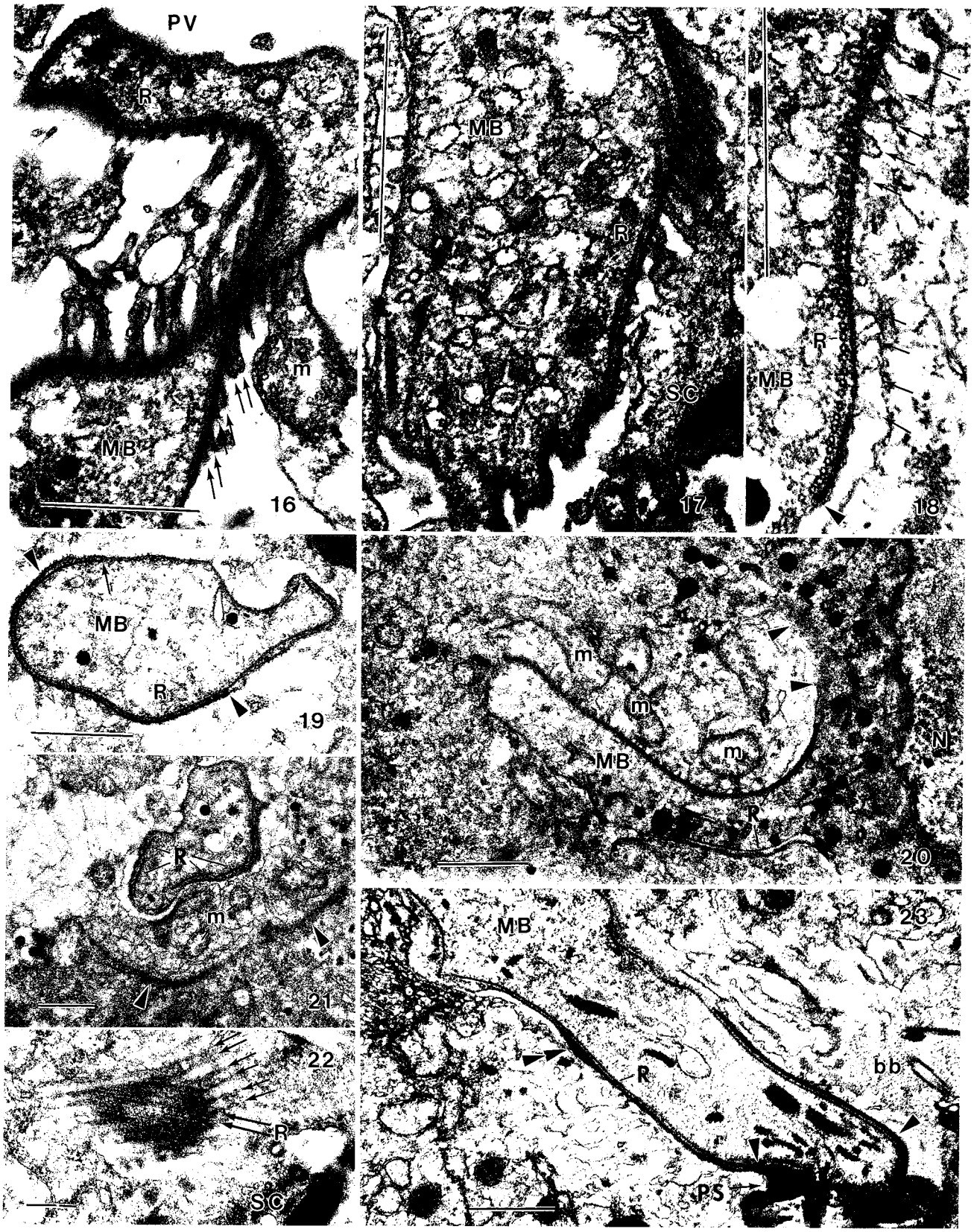

FIGS. 16–23. The microtubular basket of the pallium. FIG. 16. Vacuole-surrounded MB of feeding cell showing regularly spaced riblike channels (arrows). FIG. 17. Base of MB (same cell as Fig. 2) showing regularly spaced channels and numerous vesicles within pallioplasm. FIG. 18. Apical MB (enlargement of Fig. 2, upper arrowhead) showing electron-dense layer (arrowhead) adjacent to microtubular ribbon and membrane channels (arrows). FIG. 19. Cross section of distal region of MB with single microtubular ribbon

son 1987, Shapiro et al. 1989). The extended pallium, however, has no detectible autofluorescence. In other words, the autofluorescent material, though widely distributed within the cytoplasm, is somehow excluded from the pallium.

Situated at the base of the MB is an osmiophilic ring, which we term the pallial sphincter, through which the pallioplasm proceeds. This electron-dense structure is doughnut or torus-like (Figs. 9, 35, 45). The sphincter is nearly amorphous, although corrugations on its outer surface (Fig. 45) and striations (Fig. 36) are barely discernible. An electron-lucent membrane-bound fibrillar region, which we term the corona, surrounds the pallial sphincter (Figs. 9, 25, 35, 45). This feature was seen in all (five) *P. spinulosum* cells whose pallial sphincters were examined, but not in *P. punctulatum.*

Two nonfeeding cells (one from each of the two fixation protocols) were examined. The MB was found in both cells, although the ordered membranous invaginations were not observed. In one, the MB is surrounded by a large pallial vacuole (Fig. 24). In addition to the longitudinal flagellum (not shown), a cytoplasmic protrusion with a barely discernible peripheral row of microtubules and an elaborate outer glycocalyx (Figs. 24, 26) is located within the sulcus.

A second non-feeder was fixed while that cell was engaged in a spiralling pre-capture "dance" (Jacobson and Anderson 1986), which indicated that the cell was prepared to deploy its pallium. The cell, which was fixed with the tannic acid protocol, has a distinct ultrastructural appearance. A MB and a pallial sphincter are present, with an electron-lucent corona region (smaller than that seen in feeding cells) adjacent to the sphincter (Fig. 25). The pallial sphincter resembles those in feeding cells in having a featureless internal structure, but it is less electron dense. The sulcus is filled with an electron-dense substance that appears to be poorly embedded, resulting in uneven sectioning (Figs. 25, 30). The electron-dense mass completely fills and distends the sac pusular duct; some electron-dense material has squeezed through the striated collar of the sac pusule (Fig. 30). Concentric membrane profiles are located within the pusule. A partially obscured system of fingerprint-like whorls with a periodicity of 5 nm can be seen in this electron-dense region (Fig. 30, inset). Similar formations are also located within or adjacent to the MB but with a less-ordered structure (Figs. 28, 29) with 9-nm membrane spacings.

Most interestingly, a small lobate pseudopodal structure containing one to several rows of microtubules emerges from the mass of fingerprint structures (Fig. 25). The outer membrane of the pseudopod has a thin glycocalyx; inside this membrane are microtubules arranged in a ribbon with center-to-center distances of 35 nm (Fig. 27). The microtubules are associated with amorphous material and appear to be composed of 13 tubulin subunits.

The pallial sphincter is located at the center of a remarkably complex system of striated electron-dense connecting fibers or myonemes (Fig. 46). This system is illustrated by a set of micrographs detailing longitudinal sections through both the ventral (Figs. 31–37) and dorsal (Figs. 39–44) sides of a plane passing through the pallial sphincter. Beginning at the pallial sphincter and facing ventrally, a stout myoneme (the largest in this cell) reaches from the sphincter to the transverse flagellar duct (Fig. 35). A second major myoneme (Fig. 33) links the flagellar duct wall with the pore plate. A narrowing extension of the first myoneme is anchored to the extremity of a protrusion formed by a minute thecal plate (the anterior accessory sulcal plate, AASP) together with the posterior extremity of the anterior sulcal plate (Fig. 35). The MB rests so closely against the AASP that its contours conform to those of the latter. A short myoneme bridges the gap between the large sphincter myoneme and the striated collar of the collecting pusule (Fig. 35). A thin striated sheath lines the anterior portion of the flagellar duct adjacent to the striated collar (Fig. 35). Another sheath cups the basal chamber of the collecting pusule (Fig. 37). Ribbons of striated material hang from the mouth of the pallial sphincter, in intimate contact with the pallium (Fig. 35; see Fig. 36 for the subtle striation details).

The pore plate has a distinctive three-layer fibrous ultrastructure (Fig. 34) unlike that of all other thecal plates; it has two electron-lucent layers separated by a central electron-dense layer. This plate is actually composed of two plates (Figs. 31, 40). The electron-dense layer of the pore plate fuses with the adjacent left sulcal plate (Fig. 32); periodic bands are visible at this junction.

In addition to myonemes, a population of at least nine small (<1 μm) electron-dense organelles shows

←

(edges of ribbon: arrows) and electron-dense outer sheath (edges of sheath: arrowheads). Continuation of this MB shown in Figure 21. FIG. 20. Apical end of MB terminating adjacent to nucleus and between sac and collecting pusules (not shown). Fibrous recurved flap (arrowheads) is seen in cross section in Figure 21. FIG. 21. MB apical opening (section dorsal to Fig. 19) showing fibrous recurved flap (arrowheads), mitochondria beneath flap, and membrane-bound lipid droplets. Note discontinuous microtubular ribbons. FIG. 22. Tangential section of MB (dorsal side). Note membranous channels (short arrows) that are angled 30° from the microtubules (long arrows). The membranous channels have a somewhat beaded appearance. Two collared pits are next to striated collar. Scale bar = 100 nm. FIG. 23. MB of *Protoperidinium punctulatum.* Arrowheads indicate striated regions of electron-dense pallial sheath. Note elongate electron-dense granules and lack of pallial sphincter corona.

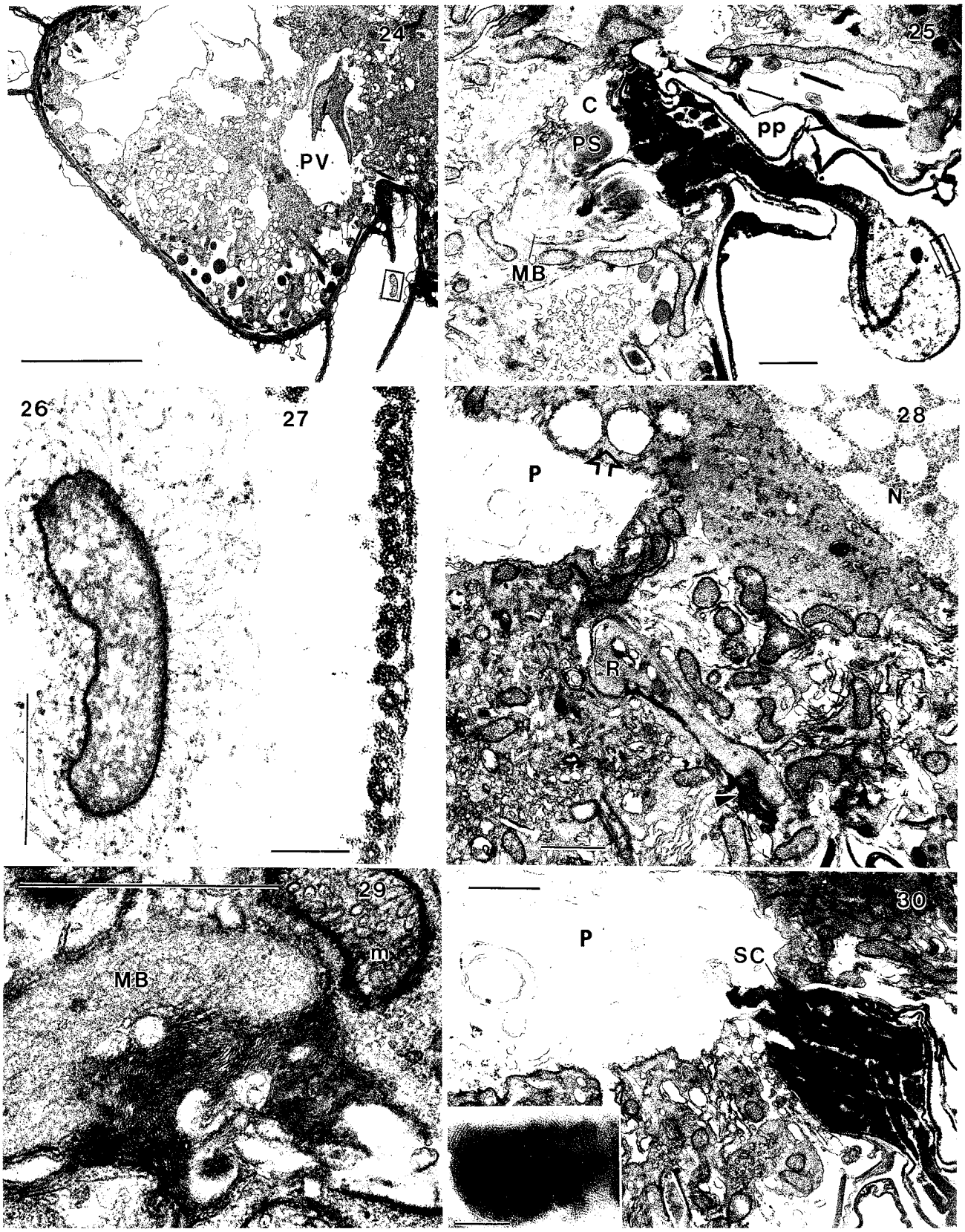

FIGS. 24–30. Nonfeeding *P. spinulosum* cells. FIG. 24. Longitudinal section showing MB (with electron-dense granule) within large pallial vacuole and a narrow filopod (box enlarged in Fig. 26). FIG. 25. Tannin-fixed "prefeeder" with small pseudopod emerging from an electron-dense mass adjacent to MB. FIG. 26. Enlarged filopod from Figure 24. Note elaborate membrane fringe. FIG. 27. Portion

a texture resembling that of a bottle brush; most of these lie adjacent to or in contact with the collecting pusule (Figs. 38, 46).

Many features described in the ventral region of the myonemal system are also encountered in the dorsal region. A ribbon-shaped myoneme, seen in cross section, stretches from the sphincter to the sac pusular striated collar (Fig. 41), through which the longitudinal flagellum passes. The striated collar is anchored by myonemal material to the tip of a thecal protrusion (Fig. 44); the latter is formed by two posterior accessory sulcal plates (PASP) and the extremity of the right sulcal plate (Figs. 43, 44). A separate, less conspicuous myonemal connection is formed between the PASP and the pallial sphincter (Figs. 41–43). This connective is especially evident in transverse section (Fig. 45). The posterior striated collar makes intimate contact with the microtubular root of the longitudinal flagellum (Fig. 43).

DISCUSSION

A coherent image of the complex feeding apparatus of *P. spinulosum* has emerged from the seven cells examined in this study. The reconstructions of the relevant organelles (Figs. 1, 46) reveal the arrangement of the MB and its sphincter adjacent to an inner thecal protuberance. Also shown are the connections between the osmiophilic ring and the striated collars, and the location of the basal bodies between the sac and collecting pusules.

The discovery of a MB in *P. spinulosum* and *P. punctulatum* (this study) and in *P. hirobis* and *Oblea rotunda* (Jacobson 1987) strongly suggests that this structure is a constant feature among species of *Protoperidinium* and the allied diplopsaloid dinoflagellates, and possibly among the pseudopod-bearing genera of *Podolampus* and *Blepharocysta* (Schütt 1895) as well. A clear homology exists between the *Protoperidinium* MB and the peduncle of some naked and thecate phagotrophic dinoflagellates. Besides the elaborate microtubular arrays that these two feeding structures have in common, shared features include the presence of an osmiophilic ring or sphincter (not found in some peduncles) where the feeding structures exit the cell and the presence of elongate electron-dense granules. Osmiophilic rings have been reported in *Gyrodinium lebouriae* (Lee 1977), *Paulsenella* sp. (Schnepf et al. 1985), and the parasite *Protoodinium chattoni* (Cachon and Cachon 1971). However, the electron-lucent fibrillar zone surrounding the osmiophilic ring in *P. spinulosum* is not seen in these other species. Elongate electron-dense bodies in *P. spinulosum, P. punctulatum,* and *Protoperidinium hirobis* (Jacobson 1987) are also seen within the peduncles of *Gymnodinium lebouriae* (Lee 1977), *Katodinium fungiforme* (Spero 1982), *Peridiniopsis berolinense* (Wedemayer and Wilcox 1984), *Paulsenella* sp. (Schnepf et al. 1985), *Amphidinium acidotum* (Wilcox and Wedemayer 1984), *Amphidinium poecilochroum* (Larsen 1988), and *Dinophysis acuminata* (Lucas and Vesk 1990). These may contain digestive enzymes. Although the mechanics of feeding in pallium and peduncle are dissimilar, the granules found in the pallioplasm resemble those found in the peduncle. One of the few organelles not shared by both peduncle and pallium are the electron-lucent microbodies found in two cells near the anterior end of the pallial MB. A microbodylike structure was seen in a pallium adjacent to a recently captured diatom (not shown), suggesting that microbodylike structures may play some role in the feeding process.

The number and arrangement of microtubules in the pallial MB fall within the large variation found among peduncular morphologies. The peduncular microtubules of some species are arranged as overlapping, semiradial ribbons, numbering 9 in *Protodinium chattoni* (Cachon and Cachon 1971), 19 in *Gymnodinium fungiforme* (Spero 1982), and 58 in *Peridiniopsis berolinense* (Wedemayer and Wilcox 1984). However, a single microtubular ribbon was found in *Amphidinium acidotum* (Wilcox and Wedemayer 1984), *Amphidinium poecilochroum* (Larsen 1988), and *Dinophysis rotunda* (unpubl. observ.). The microtubular basket of a single cell of *Protoperidinium spinulosum* can have along its length a mixture of single and multiple ribbon morphology. Further, nine distinctly overlapping microtubular ribbons occur in the MB of *P. sinuosum* (unpubl. observ.). We are unable, therefore, to correlate feeding strategy with microtubular ribbon arrangement. To underscore this conclusion, consider the attempt by Lucas and Vesk (1990) to correlate peduncular complexity with function. *Dinophysis acuminata,* they observe, has a simple peduncle-like structure with a single microtubular ribbon that they interpret as representing an atrophied condition. However, one of us has found that the peduncular ultrastructure of two related and actively phagotrophic species, *Dinophysis rotundata* and *Oxyphysis oxytoxioides,* resembles that of *D. acuminata.*

No striking distinction can yet be made between the microtubular ribbons of peduncle and pallium. However, although the peduncular MB is often embedded directly in the surrounding cytoplasm, the

---

←
of microtubular ribbon, enlargement of Figure 25 (box on pseudopod). +tannin. Scale bar = 100 nm. FIG. 28. Section dorsal to Figure 25, showing MB and adjacent dense mass (arrowhead) (enlarged in Fig. 29). Note microbodies between pusule and nucleus (arrow). +tannin. FIG. 29. Membranous whorls of MB, enlarged from section adjacent to Figure 28. +tannin. FIG. 30. Section dorsal to Figure 28 showing dense mass (composed of whorls, inset; scale bar = 100 nm) distending pusule duct and entering sac pusule through striated collar. Note membranes within normally empty pusule.

FIGS. 31–38. Section series showing myonemes and pore plate on ventral side of cytostome. FIG. 31. Pore plate and surrounding sulcal plates (ventral-most section). Note pore plate suture (arrowhead). FIG. 32. Pore plate attachment sites on left sulcal plate (arrowhead, arrows). FIG. 33. Myonemal system adjacent to pallial sphincter. Note narrow thecal plate (arrowhead = AASP) which, with anterior sulcal plate, forms thecal protuberance. FIG. 34. Enlargement of pore plate of Figure 31 showing three layers. FIG. 35. Cytostome with

pallial MB and associated pallioplasm form a discrete compartment separated from the surrounding cytoplasm by a membrane (sometimes a pleated membrane) and an electron-dense sheath. The microtubular ribbons of peduncles are often embedded directly in the cytoplasm with no limiting membrane. These ultrastructural observations are consistent with the different strategies employed by pallium and peduncle. The pallium MB transports food material that has already been liquified by digestive enzymes (which must be isolated to avoid damage to the *Protoperidinium* cytoplasm), whereas the peduncle transports large parcels of minimally altered prey cytoplasm that will later be digested within conventional food vacuoles.

Microtubular oral structures are found in a number of nondinoflagellate protists, including trichomonads, with their single microtubular row pelta–axosytle complex (Honigberg et al. 1971, Brugerolle 1980), and euglenoid flagellates, with their perireservoir microtubules (Walne 1980). None bears as close a resemblance to the MB as does the peduncle.

The regularly spaced membrane ribs or pleats associated with the MB resemble those seen adjacent to food vacuoles of the phagocytic flagellate *Gyromitus disomatus* (Swale and Belcher 1974). These latter structures were thought to be endocytotic vesicles. The MB-associated channels in *P. spinulosum* also have a beaded appearance similar to that seen in *G. disomatus* but form flattened channels instead of the regularly spaced cylindrical tubules of *G. disomatus.* The channels in both *G. disomatus* and *P. spinulosum* are 40 nm in diameter. This extensive array of channels may constitute an alternate route for the inward transport of ingested material. These channels were not seen in nonfeeding cells, but additional cells need to be examined before this difference can be considered significant.

The question of the source of the enormous quantities of membranes needed to form a pallium (enough, in some cases, to envelope a chain of diatoms several hundred micrometers in length) can now be at least partially answered. In a cell that was preparing to feed, two membranous complexes were found. One of these complexes has the form of tightly packed fingerprint-like whorls. The uneven sectioning of the sulcal region in which these patterns are found, clearly the result of a localized lack of rigidity in the embedding plastic, may, together with the fingerprint patterns, indicate the presence of lipid-rich structures. A condensed store of membranes may be accumulated near the flagellar pore prior to feeding. A possibly related membranous complex within the MB, that has a somewhat less ordered appearance, is similar to the electron-dense "rhoptry" structures observed in *Plasmodium berghei* and thought to be the storage site for membranes to be discharged outside the cell (Stewart et al. 1985). The more orderly fingerprint patterns resemble structures found in fatty acid storage sites of liver cells (Blanchette-Mackie and Amende 1987). These observations need to be supplemented by a time course through the prefeeding and pallium-deployment phases in order to more fully reveal the membrane dynamics of the feeding apparatus in *P. spinulosum.*

Our study is the first to describe the interconnectedness of the striated collars, cytostomal (pallial) sphincter, and thecal anchor sites, including the pore plate. A similar configuration (with linkages between peduncle sphincter and striated collars) has been found in a freshwater myxotroph, *Peridinium inconspicuum* (Ngo, pers. commun.). Myonemal linkages have been reported between flagellar roots and the nucleus (Bradbury et al. 1983, Roberts 1986). The myonemal system of *Kofoidinium pavillardi* is thought to be an elaboration of the striated root of the transverse flagellum; it begins at the basal body, runs around the duct of the collecting pusule, and then splits into four branches that wind around the pusule (Cachon et al. 1983). Myonemes are thought to be contractile. They display various striation periodicities, corresponding, it seems, to various states of contraction. The calcium-binding contractile protein centrin seems to be an important component of electron-dense striated fibers of some flagellates (Salisbury 1989). Cachon et al. (1983) suggest that the myonemes in *K. pavillardi* may squeeze the contents of the pusule. They also reported the periodic sudden contraction of the collecting pusule of *Protoperidinium depressum* and suggest that a myonemal structure like that in *K. pavillardi* may be able to exert a squeezing force upon the collecting pusule, resulting in forceful expulsion of its contents. However, no ultrastructural data for *P. depressum* were presented. No myonemal structures besides the striated collar encircles the collecting pusule in *Protoperidinium spinulosum.* The myonemal system of *P. depressum* clearly deserves investigation.

Several details of the pallium deserve comment. The lack of an inner membrane adjacent to the prey diatom frustule is startling. A single outer membrane seems structurally weak and vulnerable to lysis, yet an inner plasma membrane adjacent to the

←

pallium emerging from PS, four sections dorsal of Figure 33. Note extremity of thecal protuberance (arrowhead), striated collar of collecting pusule and striated layer within flagellar canal (arrow). FIG. 36. Enlargement of PS in Figure 35 detailing subtle striations adjacent to dash marks (see text). FIG. 37. Base of collecting pusule with sheath (arrowheads) extending from striated collar. FIG. 38. Collecting pusule (note sinuous tubules) adjacent to basal body of transverse flagellum and the wedge-shaped cytoplasmic region surrounding the latter (arrows). Note fibrillar lamellae (arrowheads).

FIGS. 39–45. Section series showing continuity of myonemes on dorsal side of cytostome. FIG. 39. Dorsal part of pallial sphincter, from which two connectives originate. FIG. 40. Five sections dorsal to Figure 39. Suture divides pore plate (arrowhead). FIG. 41. One connective (arrowhead) stretches toward striated collar of sac pusule; another connective (arrow) reaches toward thecal protuberance. Striations are visible on inner surface of pore plate (dash marks). FIG. 42. First connective has joined striated collar; second connective has flattened cross section (arrow). FIG. 43. Second connective contacts tapered thecal protuberance. Microtubular root of the longitudinal flagellum makes contact with striated collar. FIG. 44. Striated material (arrow) anchors striated collar to tip of thecal protuberance. FIG. 45. Transverse section through pallial sphincter, showing connective between sphincter and thecal protuberance. Lumen of sphincter (marked by white dots) is occupied by very electron-dense pallioplasm. Regular, diminutive ridges occur on pallial sphincter (dash marks). Note surrounding corona region.

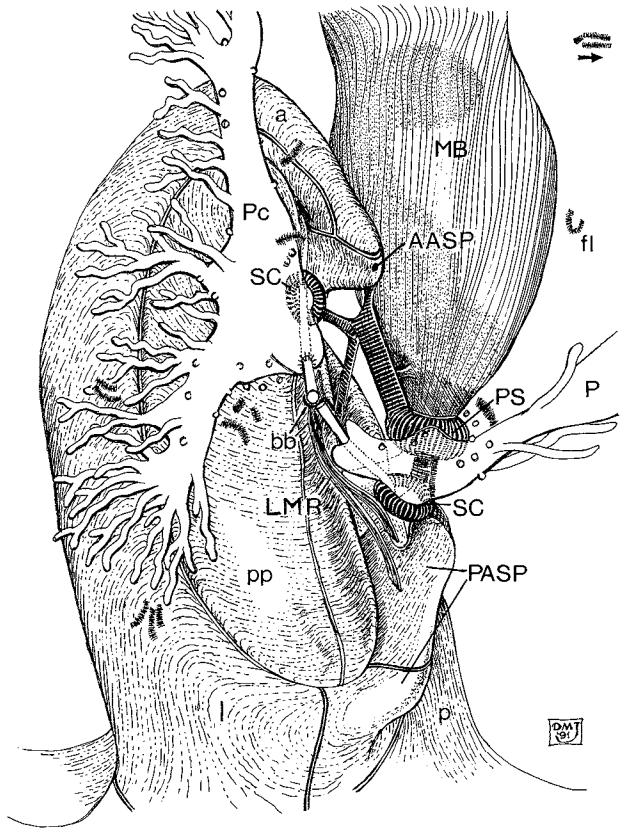

FIG. 46. Diagrammatic reconstruction of myonemal and pusular systems surrounding MB illustrating their relation to the two thecal protuberances. For simplicity the transverse flagellar duct with its striated inner sheath is not included. Note collared pits near pusules and fibrillar lamellae, most of which occur near collecting pusule. One fl is located 1 μm off to the right.

prey diatom was only observed in the pallium of one cell. Only a single outer membrane was present in two other feeding cells, enclosing a multitude of empty vesicles (many of which are closely appressed to the outer membrane) next to the frustule. Either the putative inner membrane was destroyed during fixation, perhaps becoming artifactually reorganized as a series of small vesicles, or it so reorganizes *in vivo*. This situation needs further investigation, utilizing carefully adjusted fixation techniques that would prevent any extraction of cytoplasmic components.

Before the pallium is deployed, the prey item is captured at the end of a filopod called the tow filament (Jacobson and Anderson 1986). The slender pseudopodia in two nonfeeding cells (including, importantly, a cell fixed during capture behavior) can be provisionally identified as tow filaments. The microtubular ribbon(s) in one of these pseudopodia may be involved in the pseudopodal contraction observed in the moments following prey capture. The elaborate glycocalyx of the other pseudopod may give the filopod an adhesive quality that would be crucial for the capture of motile prey. This elaborate glycocalyx resembles that found on the stalk of a fully deployed pallium and may have a common origin.

The apparent attachment of a myonemal connective to the pore plate invites speculation on possible structural dynamics. We have shown that this pore plate, also known as the median sulcal plate, has a unique fibrous composition and a concave boat-shaped form. Balech (1974) described it as a "membranous" (i.e. very thin) ovoid structure. Perhaps the pore plate deforms in response to forces exerted by the myonemal connective, thereby modulating the diameter of the posterior flagellar pore. This idea is supported by the presence of dome-shaped pore plates positioned operculumlike at the cytostome of *Oxyphysis oxytoxoides* and *Dinophysis rotundata* (pers. observ.). These thecate dinoflagellates ingest large parcels of cytoplasm taken from their ciliate prey through their flexible peduncles. The pore plate clearly must be collapsed or pushed aside as the large food vacuoles pass through the cytostome. Such an adaptation may be advantageous to a dinoflagellate endeavoring to reduce the duration of pallium deployment or retraction.

We thank O. R. Anderson for his valuable suggestions and D. K. Stoecker for use of her rotating apparatus. This work was supported by the Woods Hole Oceanographic Institution Education Office and National Science Foundation grants OCE-8400292 and OCE-8911226. This is contribution no. 91017 from the Bigelow Laboratory for Ocean Sciences and contribution no. 7713 from the Woods Hole Oceanographic Institution.

Balech, E. 1974. El genero "Protoperidinium" Bergh, 1881 ("Peridinium" Ehrenberg 1831, Partim). *Rev. Mus. Argent. Cienc. Nat. 'Bernardino Rivadavia' Inst. Nac. Invest. Cienc. Nat. B. Aires Cienc. Bot.* 4:1–79.

Blanchette-Mackie, E. J. & Amende, L. M. 1987. Electron microscopic visualization of fatty acids in tissues. *J. Electron Microsc. Tech.* 7:205–21.

Bradbury, P. C., Westfall, J. A. & Townsend, J. W. 1983. Ultrastructure of the dinoflagellate *Polykrikos*. II. The nucleus and its connection to the flagellar apparatus. *J. Ultrastr. Res.* 85:24–32.

Brugerolle, G. 1980. Étude ultrastructurale du flagellé *Protrichomonas legeri* (Léger 1905), Parasite de l'estomac des bogues (Box boops). *Protistologica* 16:353–8.

Cachon, J. & Cachon, M. 1971. *Protoodinium chattoni* Hovasse. Manifestations ultrastructurales des rapports entre le Peridinien et la Meduse-hote: fixation, phagocytose. *Arch. Protistenkd.* 113:293–305.

Cachon, J., Cachon, M. & Boillot, A. 1983. Flagellar rootlets as myonemal elements for pusule contractility in dinoflagellates. *Cell Motil.* 3:61–77.

Calkins, G. 1901. *The Protozoa.* Macmillan Co., New York, 347 pp.

Dodge, J. D. 1971. Fine structure of the Pyrrophyta. *Bot. Rev.* 37:481–507.

Dodge, J. D. & Crawford, R. M. 1970. The morphology and fine structure of *Ceratium hirundinella* (Dinophyceae). *J. Phycol.* 6:137–49.

Gaines, G. & Taylor, F. J. R. 1984. Extracellular feeding in marine dinoflagellates. *J. Plankton Res.* 6:1057–61.

Guillard, R. R. L. & Ryther, J. H. 1962. Studies of marine planktonic diatoms. I. *Cyclotella nana* Hustedt and *Detonula confervacea* (Cleve). *Can. J. Microbiol.* 8:229–39.

Honigberg, B. M., Mattern, C. F. T. & Daniel, W. A. 1971. Fine structure of the mastigont system in *Tritrichomonas foetus* (Riedmuller). *J. Protozool.* 18:183–98.

Jacobson, D. M. 1987. The ecology and feeding biology of thecate heterotrophic dinoflagellates. Ph.D. thesis, Woods Hole Oceanographic Institution/Massachusetts Institute of Technology Joint Program, 210 pp.

Jacobson, D. M. & Anderson, D. M. 1986. Thecate heterotrophic dinoflagellates: feeding behavior and mechanisms. *J. Phycol.* 22:258–69.

Knobler, R. L., Stempak, G. J. & Laurenein, M. 1978. Preparation and analysis of serial sections in electron microscopy. *In* Hayat, M. A. [Ed.] *Principles and Techniques of Electron Microscopy,* Vol. 8. Van Nostrand Reinhold, New York, pp. 113–55.

Larsen, J. 1988. An ultrastructural study of *Amphidinium poecilochroum* (Dinophyceae), a phagotrophic dinoflagellate feeding on small species of cryptophytes. *Phycologia* 27:366–77.

Lee, R. E. 1977. Saprophytic and phagocytic isolates of the colourless heterotrophic dinoflagellate *Gyrodinium lebouriae* Herdman. *J. Mar. Biol. Assoc. U.K.* 57:303–15.

Lucas, I. A. N. & Vesk, M. 1990. The fine structure of two photosynthetic species of *Dinophysis* (Dinophysiales, Dinophyceae). *J. Phycol.* 26:345–57.

Morey-Gaines, G. & Elbrachter, M. 1987. Hetrotrophic nutrition. *In* Taylor, F. J. R. [Ed.] *The Biology of Dinoflagellates.* Blackwell Scientific, Oxford, pp. 224–69.

Neveux, J. & Soyer, M. O. 1976. Charactérization des pigments et structure fine de *Protoperidinium ovatum* Pouchet (Dinoflagellata). *Vie Milieu* 26:175–99.

Roberts, K. 1986. The flagellar apparatus of *Gymnodinium* sp. (Dinophyceae). *J. Phycol.* 22:456–66.

Salisbury, J. L. 1989. Centrin and the algal flagellar apparatus. *J. Phycol.* 25:201–6.

Schnepf, E., Deichgräber, G. & Drebes, G. 1985. Food uptake and the fine structure of the dinophyte *Paulsenella* sp., an ectoparasite of marine diatoms. *Protoplasma* 124:188–204.

Schnepf, E & Winter, S. 1990. A microtubular basket in the armoured dinoflagellate *Prorocentrum micans* (Dinophyceae). *Arch. Protistenkd.* 138:89–91.

Schütt, F. 1895. *Die Peridineen der Plankton-Expedition.* Lipsius and Tischer, Kiel, Germany, 170 pp.

Shapiro, L. P., Haugen, E. M. & Carpenter, E. J. 1989. Occurrence and abundance of green-fluorescing dinoflagellates in surface waters of the northwest Atlantic and northeast Pacific oceans. *J. Phycol.* 25:189–91.

Simionescu, N. & Simionescu, M. 1976. Galloylglucoses of low molecular weight as mordant in electron microscopy. *J. Cell Biol.* 70:608–21.

Spector, D. L., Pfiester, L. A. & Triemer, R. E. 1981. Ultrastructure of the dinoflagellate *Peridinium cinctum* f. *ovoplanum.* II. Light and electron microscopic observations on fertilization. *Am. J. Bot.* 68:34–43.

Spero, H. J. 1982. Phagotrophy in *Gymnodinium fungiforme* (Pyrrophyta): the peduncle as an organelle of ingestion. *J. Phycol.* 18:356–60.

Spurr, A. R. 1969. A low viscosity epoxy embedding medium for electron microscopy. *J. Ultrastruct. Res.* 26:31–43.

Stewart, M. J., Schulman, S. & Vanderberg, J. P. 1985. Rhoptry secretion of membranous whorls by *Plasmodium berghei* sporozoites. *J. Protozool.* 32:280–3.

Swale, E. M. F. & Belcher, J. W. 1974. *Gyromitus disomatus* Skuja—a free-living colourless flagellate. *Arch. Protistenkd.* 116:211–20.

Walne, P. L. 1980. Euglenoid flagellates. *In* Cox, E. R. [Ed.] *Phytoflagellates.* Elsevier/North-Holland, New York, pp. 165–212.

Wedemayer, G. J. & Wilcox, L. W. 1984. The ultrastructure of the freshwater, colorless dinoflagellate *Peridiniopsis berolinense* (Lemm) Bourrelly (Mastigophora, Dinoflagellida). *J. Protozool.* 31:444–53.

Wilcox, L. W. & Wedemayer, G. J. 1984. *Gymnodinium acidotum* Nygaard (Pyrrophyta), a dinoflagellate with an endosymbiotic cryptomonad. *J. Phycol.* 20:236–42.